[CANCER RESEARCH 58, 3620–3626, August 15, 1998]

Mechanisms of Taxol-induced Cell Death Are Concentration Dependent[1]

Keila Torres and Susan Band Horwitz[2]

Department of Molecular Pharmacology, Albert Einstein College of Medicine, Bronx, New York 10461

ABSTRACT

Although the ability of Taxol to stabilize cellular microtubules is well accepted, the mechanisms by which Taxol induces growth arrest and cell death remain unclear. Recent evidence indicates that Taxol alters specific intracellular signal transduction events, such as the activation of Raf-1 kinase, that may be essential for drug-induced apoptosis. To determine whether Raf-1 kinase activation occurs at different concentrations of Taxol and in response to disruption of the normal microtubule cytoskeleton, A549 cells were treated with different concentrations of Taxol after which Raf-1 activation and the microtubule cytoskeleton were analyzed. Raf-1 activation was observed at Taxol concentrations of 9 nM and greater. However, disruption of the normal microtubule cytoskeleton was seen at lower Taxol concentrations (1–7 nM), indicating that this process begins in the absence of Raf-1 activation. Raf-1 activation correlated with the induction of a G_2-M block. Depletion of Raf-1 resulted in the accumulation of cells in the G_2-M phase of the cell cycle, suggesting that Raf-1 may play an important role in the passage through mitosis. Supporting this idea, Raf-1 was activated in mitotic cells. Low concentrations of Taxol induced cell death in the absence of Raf-1 activation, indicating that Taxol-induced cell death is not dependent on Raf-1 activation. At concentrations of drug lower than the critical concentration required for Raf-1 activation, p53 and $p21^{WAF-1}$ were induced independently of Raf-1. These studies suggest that Taxol-mediated cell death may result from two different mechanisms. At low Taxol concentrations (<9 nM), cell death may occur after an aberrant mitosis by a Raf-1 independent pathway, whereas at higher Taxol concentrations (≥9 nM) cell death may be the result of a terminal mitotic arrest occurring by a Raf-1-dependent pathway.

INTRODUCTION

Taxol has significant antitumor activity in several human tumors, particularly in advanced ovarian, lung, and breast carcinomas (1). The cellular target for Taxol has been identified as the tubulin/microtubule system (2) that plays a significant role in mitosis, intracellular transport, cell motility, and maintenance of cell shape. Taxol promotes the assembly of stable microtubules from α- and β-tubulin heterodimers and inhibits their depolymerization (3). Although the interaction of Taxol with β-tubulin is well characterized (4, 5), the molecular mechanisms by which such interactions may lead to cell cycle arrest and cell death are not clear.

Incubation of cells with high Taxol concentrations leads to the formation of stable bundles of microtubules that disrupt the normal polymerization/depolymerization cycle of microtubules and results in the arrest of cells in the G_2-M phase of the cell cycle (6). In addition to massive bundle formation, increased microtubule polymer mass is observed after treatment with high concentrations of Taxol (7). However, low concentrations of Taxol (10 nM) inhibit mitosis in HeLa cells by suppressing microtubule dynamics rather than by altering the microtubule polymer mass or inducing bundle formation (7). The mitotic block induced by 10 nM Taxol is sufficient to induce apoptosis (8). These observations in HeLa cells indicate that Taxol-induced cell death may result from different mechanisms depending on drug concentration.

Specific intracellular signal transduction events are altered by Taxol. It has been reported that Taxol induces the production of cytokines, interleukin-1, and tumor necrosis factor α and increases tyrosine phosphorylation of proteins, including mitogen-activated protein kinase (9–13). Prolonged exposure of cells to Taxol induces DNA fragmentation, characteristic of apoptotic cell death (14), and recent work has suggested that Raf-1 is a mediator of Taxol-induced apoptosis (15, 16). Raf-1 is known as an important intermediate in the transmission of proliferative and developmental signals, connecting upstream tyrosine kinases with downstream serine/threonine kinases (17). It is not clear whether Raf-1 activation is a consequence of disruption of the normal microtubule cytoskeleton and/or of activating the spindle mitotic checkpoint.

To determine whether cell death induced by Taxol resulted from a single mechanism or different mechanisms related to drug concentration, several questions have been explored: (*a*) Is Raf-1 activation an important step in the induction of cell death at low concentrations of Taxol? (*b*) Is a critical level of microtubule disruption required for Raf-1 activation? and (*c*) How does the critical drug concentration necessary for Raf-1 activation correlate with Taxol-induced cell cycle disruption? To address these questions, a human Taxol-sensitive lung carcinoma cell line, A549, was treated for 18 h with different concentrations of Taxol, ranging from 1–250 nM. After treatment, DNA content, activation of Raf-1, subcellular organization of microtubules, and nuclear morphology were studied.

The present work reveals that microtubule and cell cycle disruption occur at very low concentrations (<9 nM) of Taxol. The minimum Taxol concentration necessary for Raf-1 activation coincides with the minimum concentration required to induce a G_2-M block, suggesting that Raf-1 activation is related to the accumulation of cells in the G_2-M phase. However, Raf-1 activation is not required for cell death. At low Taxol concentrations, p53 and $p21^{WAF-1}$ induction is independent of Raf-1 activation. Microtubule alterations occur even at the lowest concentration of Taxol (1 nM) that was studied. The data reported here suggest that Taxol can induce cell death by two different mechanisms, depending on drug concentration. At low Taxol concentrations, a Raf-1-independent pathway is activated, whereas at higher Taxol concentrations, a Raf-1-dependent pathway is activated.

MATERIALS AND METHODS

Cell Culture. Human non-small cell lung carcinoma cells, A549, were maintained in RPMI 1640 containing 1% penicillin-streptomycin (Life Technologies, Inc., Grand Island, NY) and 10% fetal bovine serum (Life Technologies, Inc.). Cells were grown as monolayer cultures in 7% CO_2 and passaged at intervals of 3 days.

Reagents. Taxol was obtained from the Drug Development Branch, National Cancer Institute (Bethesda, MD), and geldanamycin was from Life Technologies, Inc. Stock solutions of both drugs, 1 mM, were prepared in 100% DMSO. Polyclonal anti-$p21^{WAF-1}$, monoclonal anti-p53, and polyclonal anti-Raf-1(C-12) antibodies were purchased from Santa Cruz Biotechnology (Santa Cruz, CA); monoclonal anti-c-Raf-1 antibody was purchased from Transduction Laboratories (Lexington, KY), and monoclonal β-tubulin antibody was purchased from Sigma Chemical Co. (St. Louis, MO). Horseradish-peroxidase-conjugated antirabbit or antimouse antibodies and enhanced chemi-

Received 2/6/98; accepted 6/11/98.

The costs of publication of this article were defrayed in part by the payment of page charges. This article must therefore be hereby marked *advertisement* in accordance with 18 U.S.C. Section 1734 solely to indicate this fact.

[1] Supported by NCI Grant CA39821, NCI Cancer Core Grant CA13330, and by the National Cancer Institute Training Program in Viral Oncology and Tumor Biology Grant 2T32 CA09060 (to K. T.).

[2] To whom requests for reprints should be addressed, at Department of Molecular Pharmacology, Albert Einstein College of Medicine, 1300 Morris Park Avenue, Bronx, NY 10461.

luminescence Western blotting kits were obtained from Amersham Corp. (Lexington Heights, IL). HBSS was purchased from Life Technologies, Inc. The Bio-Rad protein assay reagent and Tween 20 were purchased from Bio-Rad (Hercules, CA). Pierce colorimetric PKC assay kit Spinzyme Format and protein kinase C were purchased from Pierce Chemical Co. (Rockford, IL). All other chemicals were purchased from Sigma Chemical Co.

Flow Cytometry. Progression of cells through the cell cycle was examined by flow cytometry. A549 cells were trypsinized, collected by centrifugation, resuspended in HBSS, and fixed in 70% ethanol at 4°C for 1 h. After centrifugation, the cells were incubated for 5 min at room temperature in 1 ml of HBSS and 0.5 ml of phosphate-citric acid buffer (0.2 M Na_2HPO_4, 4 mM citric acid, pH 7.8). Cells were centrifuged and resuspended in 1 ml of HBSS containing 20 μg/ml propidium iodide and 5 Kunitz units of DNase-free RNase A. The cells were incubated at 37°C for 30 min, and DNA content was determined using a FACS[3] flow cytometer equipped with an argon-ion laser tuned to 488 nm. Forward, orthogonal light scatter and red fluorescence were measured. The sample size was ≥10,000 cells. Cell sorting was performed on a FACStar Plus (Becton Dickinson Immunocytometry Systems, San Jose, CA). The samples to be sorted were prepared as described above. Stained nuclei were excited at a wavelength of 488 nm at an intensity of 60 mw. The cells were analyzed for DNA content using pulse processing, so that the integrated area of the DNA fluorescence pulse was displayed as a frequency distribution of DNA content. A dual-parameter dot plot of fluorescence width *versus* fluorescence area was displayed to allow the exclusion of cell aggregates from analysis. Sort regions were defined on a fluorescence area histogram so that the cells to the left of the G0/G1 peak (hypodiploid) were isolated as the presumed apoptotic population.

Immunofluorescence Microscopy. A549 cells were grown for 24 h to subconfluency on glass coverslips in 35-mm plastic Petri dishes in complete medium. Taxol was added after 24 h, and the cells were further incubated for 18 h. Cells were rinsed with PBS and extracted for 4 min with 0.5% Triton X-100 in microtubule stabilizing buffer PEM (2 mM EGTA, 2 mM $MgCl_2$, 100 mM PIPES, pH 6.8). The coverslips were washed twice in PEM buffer, fixed for 30 min at room temperature in 3% formaldehyde in PEM, and rinsed four times in PEM buffer containing 5 μM EGTA. After blocking nonspecific binding with 5% BSA in PBS for 1 h at 37°C, cells were washed four times in PBS, incubated for 1 h at 37°C with monoclonal β-tubulin antibody (1:200 dilution in PBS), and washed with PBS four times. The slides were mounted in 50% glycerol in PBS containing 1 mg/ml β-phenylene diamine and 10 μM $MgCl_2$ and analyzed with a Zeiss Axioskop. Photographs were taken on Tmax-400 Kodak film.

Cell Viability and Cytological Techniques. After drug treatment, all of the cells (adherent and nonadherent) were harvested. Viability was estimated as the proportion of cells that excluded 0.2% trypan blue. For morphological determination of the proportion of apoptotic, multinucleated, and mitotic cells, 10,000 cells were spun onto a microscope slide (Cytospin 2; Shandon Southern Products, Ltd., Runcorn, England) and stained with Wright/Giemsa (18). One thousand cells were counted for each data point/experiment. Enlarged cells that contained multiple evenly stained nuclear fragments were considered to have undergone multinucleation. Cells that were shrunken and contained vacuolated cytoplasm and regions of intense chromatin staining were scored as apoptotic.

Analysis of Raf-1 Activation and p53 and $p21^{WAF-1}$ Expression. Cell extracts were prepared with boiling lysis buffer (1% Triton X-100 and 10 mM Tris-HCl, pH 7.4), and protein concentration was determined with the Bio-Rad protein assay reagent. Equal amounts of protein were analyzed by SDS-PAGE on 8% gels, transferred to nitrocellulose by electroblotting, and probed with monoclonal anti-c-Raf-1 (1:1000 dilution in 100 mM NaCl, 0.1% Tween 20, 1% BSA, 10 mM Tris-HCl, pH 7.4). After a 1-h incubation with the primary antibody, blots were washed, incubated with peroxidase-conjugated secondary antibody (1:500 dilution in 100 mM NaCl, 0.1% Tween 20, 1% milk, 10 mM Tris-HCl, pH 7.4), and developed using the enhanced chemiluminescence procedure (13). To determine p53 and $p21^{WAF-1}$ expression, cells were lysed in ice-cold radioimmunoprecipitation assay buffer (150 mM NaCl, 1% NP40, 0.5% sodium deoxycholate, 0.1% SDS, 1 μg/ml aprotinin, 1 μg/ml PMSF, 1 μM DTT, 50 mM Tris-HCl, pH 7.5) for 30 min at 4°C. Equal amounts of protein were analyzed by SDS-PAGE on 13% gels, transferred to nitrocellulose by electroblotting, probed with monoclonal anti-p53 (1:1000 dilution in 150 mM NaCl, 0.05% Tween 20, 10 mM Tris-HCl, pH 8.0) or with polyclonal anti-$p21^{WAF-1}$ (1:1000 dilution in 100 mM NaCl, 0.1% Tween 20, 1% BSA, 10 mM Tris-HCl, pH 7.4), and processed as above. The intensity of the bands was quantified by computerized densitometry using image analysis software.

Raf-1 Kinase Assay. Cells were trypsinized and resuspended in 10 ml of PBS. Five × 10^6 cells were lysed during incubation for 1 h at 4°C in lysis buffer containing 50 mM Tris-HCl pH 7.4, 250 mM NaCl, 5 mM EDTA, 50 mM NaF, 0.1% Nonident p-40, 2 mM sodium orthovanadate pH 10, 1 mM PMSF, 10 μg/ml leupeptin, and 10 μg/ml aprotinin. Cells were passed through a 25-gauge needle at least 10 times. The cell lysate was centrifuged at 12,000 rpm for 10 min. The resulting supernatant was immunoprecipitated overnight with 5 μl of polyclonal Raf-1 agarose conjugated antibody at 4°C. The beads were collected by centrifugation at 2500 rpm for 5 min at 4°C and washed with 1 ml of buffer containing 20 mM Hepes, pH 7.5, 4 mM EGTA, pH 8.0, 20 mM β-glycerophospate, 2 mM $MgCl_2$, 1 mM DTT, 1 mM PMSF, 10 μg/ml leupeptin, and 10 μg/ml aprotinin. Samples were resuspended in 200 μl of the buffer described above and kept on ice. Raf-1 kinase activity was determined in 10 μl of the sample suspension by using the Pierce Colorimetric PKC assay kit Spinzyme Format, according to the manufacturer's instructions. The fluorescence intensity (excitation 573 nm, emission 589 nm, 2.5 nm window) was determined by fluorescence spectroscopy. For each Raf-1 kinase determination, purified protein kinase C was used to construct a standard curve for phosphorylated substrate generated/unit of kinase activity.

RESULTS

Disruption of the Cell Cycle by Low Concentrations of Taxol. A549 cells, a highly Taxol-sensitive cell line with an ID_{50} of 2 nM, were incubated with Taxol for 18 h at concentrations ranging from 1–250 nM and analyzed by FACS. Incubation of A549 cells with low concentrations of Taxol (3–7 nM) resulted in a dose-dependent accumulation of hypodiploid cells, with a maximum effect at 5 nM (30% of the cells; Fig. 1*A*). After treatment with as little as 1–3 nM of drug, a significant percentage of hypodiploid cells was observed. After incubation with concentrations of 9–12 nM and higher, 90% of the cells were arrested at G_2-M with a 4n content of DNA (Fig. 1*A*). To determine whether high (>12 nM) Taxol concentrations were toxic after the initial G_2-M block, cells were incubated with 12 nM Taxol for longer time periods (Fig. 1*B*). Cell death was followed by the appearance of hypodiploid cells after 20, 24, and 48 h, indicating that cell death was induced after the G_2-M block.

Alterations of the Electrophoretic Mobility of Raf-1 after Taxol Treatment. To investigate whether there was a correlation between Raf-1 activation and microtubule disruption, Raf-1 gel electrophoretic mobility was examined after incubating A549 cells with different concentrations of Taxol for 18 h. Raf-1 activation is associated with hyperphosphorylation on serine residues, which results in a retardation of Raf-1 electrophoretic mobility on SDS-polyacrylamide gels (19–21). Analysis of Raf-1 activation after Taxol treatment indicated that by 9 nM of drug, a reduction in electrophoretic mobility was visible (Fig. 2*A*). This Raf-1 retardation increased after treatment with higher Taxol concentrations. At concentrations <9 nM, Raf-1 retardation was not observed. The same results were observed after incubation for 24 h.

To address whether the decreased electrophoretic mobility was indeed an activated form of the Raf-1 kinase, Raf-1 activity was directly determined by measuring the amount of phosphorylated substrate. Examination of Raf-1 kinase activity after drug treatment demonstrated a correlation between kinase activity and reduction in the electrophoretic mobility of Raf-1. At 5 nM Taxol, no significant increase in kinase activity was observed. A 2-fold increase in activity was induced after a 12 nM Taxol treatment, and a 4-fold increase could be detected after treatment with 500 nM Taxol.

The minimum Taxol concentration required for Raf-1 activation

[3] The abbreviations used are: FACS, fluorescence-activated cell sorting; PMSF, phenylmethylsulfonyl flouride.

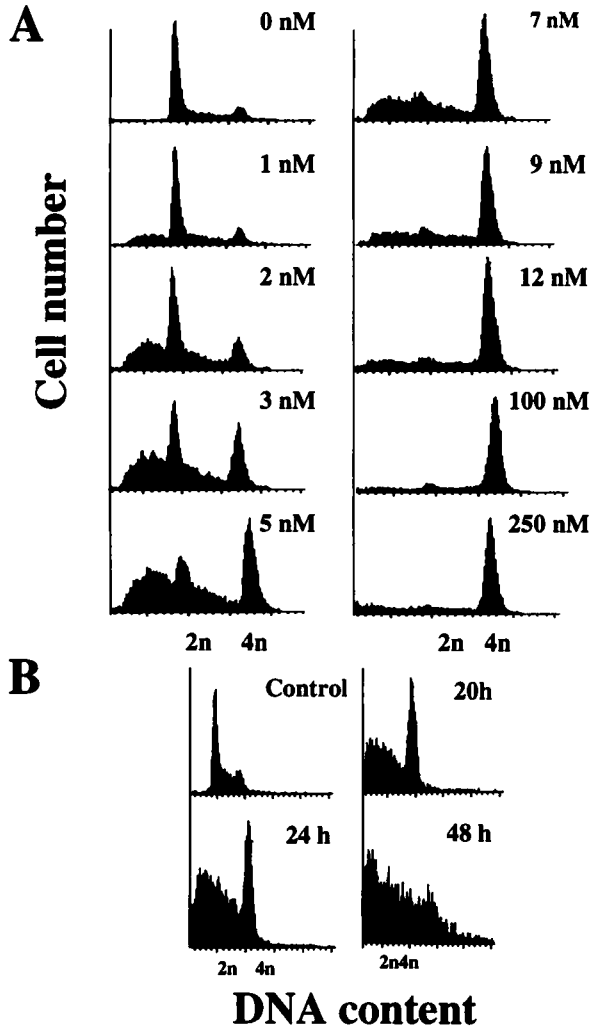

Fig. 1. Effect of Taxol on cell cycle progression in A549 cells. *A*, cells were incubated for 18 h with different concentrations of Taxol, ranging from 1–250 nM. *B*, cells were incubated with 12 nM Taxol for the indicated times. Cells were fixed, stained with propidium iodide, and analyzed by flow cytometry, as described in "Materials and Methods."

coincided with the minimum concentration needed to induce a G_2-M block, suggesting that there may be a relationship between Raf-1 phosphorylation and a G_2-M block. To determine whether Raf-1 activation was related to the accumulation of cells in G_2-M, mitotic cells were collected by mechanical shake-off. Western blot analysis demonstrated that Raf-1 mobility is retarded in mitotic cells compared with the adherent monolayer cells remaining after the shake-off (Fig. 2*C*). Less retardation of Raf-1 was observed in mitotic cells compared with normal cells treated with Taxol (Fig. 2*A*), due to the heterogeneity of the shake-off population as previously noted (20). A 3-fold increase in kinase activity was detected in mitotic cells (data not shown). An approximate 3-fold reduction in Raf-1 expression was observed in the mitotic population compared with the adherent monolayer cells.

Expression of p53 and $p21^{WAF-1}$ after Taxol Treatment. It has been demonstrated that induction of the tumor suppressor, p53, and the cyclin/cyclin-dependent kinase inhibitor, $p21^{WAF-1}$, by high Taxol concentrations, is dependent on Raf-1 activation (22). To determine whether the expression of these two proteins was altered by low Taxol levels, A549 cells were incubated with different concentrations of Taxol for 18 h. There was a parallel accumulation of both p53 and $p21^{WAF-1}$, with a maximum expression between 3–9 nM (Fig. 3*A*). At 5 nM, both proteins demonstrated an approximate 3-fold increase over the control values. This increased expression of p53 and $p21^{WAF-1}$ correlated with an increase in hypodiploid cells (Fig. 1) and suggests a role for $p21^{WAF-1}$ and p53 in mediating at least some of the cellular effects of low concentrations of Taxol.

Because our data indicate that Raf-1 mobility is not altered in the presence of <9 nM Taxol, we questioned whether the induction of p53 and $p21^{WAF-1}$ by low Taxol concentrations was dependent on the presence of Raf-1 in the cell. The benzoquinone ansamycin, geldanamycin, which binds specifically to hsp90, resulting in the disruption of a protein complex containing Raf-1, hsp90, and p50, was used to deplete the cells of Raf-1 (19, 23). Disruption of this complex results in the destabilization and degradation of Raf-1 (23). Depletion of Raf-1 did not inhibit either p53 or $p21^{WAF-1}$ induction by low levels of Taxol (Fig. 3*B*). Depletion of Raf-1 protein in the cell was confirmed by Western blotting (data not shown). The data indicate that at <9 nM Taxol, p53, and $p21^{WAF-1}$ induction was not dependent on Raf-1.

Cell Cycle Effects Induced by Taxol in the Absence of Raf-1. A549 cells were incubated either with Taxol, geldanamycin (2 μM), or with Taxol plus geldanamycin for 18 h. Geldanamycin itself caused an accumulation of cells in G_2-M after 18 h (Fig. 4), suggesting the importance of Raf-1 in the passage through mitosis. No toxicity was observed after geldanamycin treatment as determined by trypan blue staining (data not shown). Exposure of cells to geldanamycin inhibited the accumulation of hypodiploid cells induced by 5 nM Taxol, how-

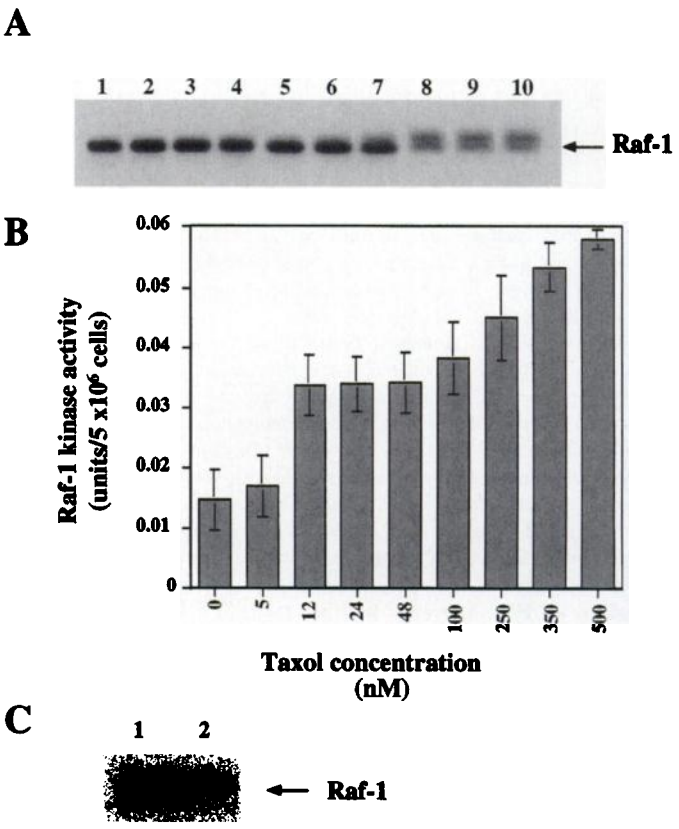

Fig. 2. Induction of Raf-1 kinase activity by Taxol. *A*, electrophoretic mobility of Raf-1. A549 cells were incubated for 18 h with different concentrations of Taxol, ranging from 1–250 nM. *Lane 1*, control; *Lane 2*, 1 nM Taxol; *Lane 3*, 3 nM; *Lane 4*, 5 nM; *Lane 5*, 7 nM; *Lane 6*, 9 nM; *Lane 7*, 12 nM; *Lane 8*, 24 nM; *Lane 9*, 100 nM; *Lane 10*, 250 nM. *B*, Raf-1 kinase activity. Kinase activity was determined as described in "Materials and Methods." The results represent three independent experiments, each done in duplicate. *C*, *Lane 1*, adherent monolayer cells remaining after mechanical shake-off; *Lane 2*, mitotic cells obtained by shake-off. Cell lysates were prepared with boiling lysis buffer. Equal amounts of total protein (30 μg) were analyzed by SDS-PAGE on an 8% gel, transferred to nitrocellulose by electroblotting, and probed with a monoclonal anti-c-Raf-1, as described in "Materials and Methods."

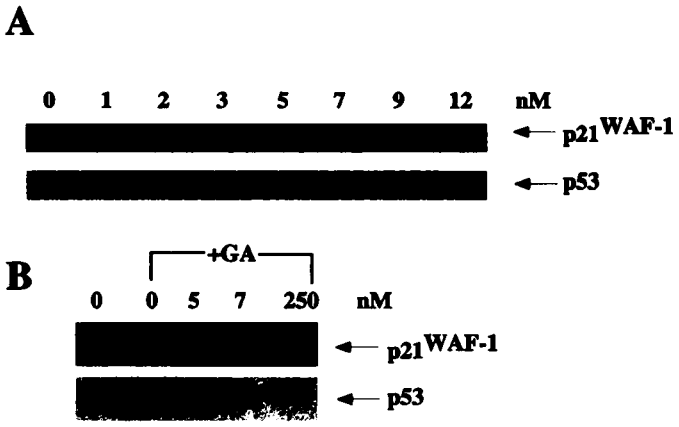

Fig. 3. Induction of the tumor suppressor p53 and cyclin/cyclin-dependent kinase inhibitor $p21^{WAF-1}$ by low Taxol concentrations. *A*, A549 cells were exposed to the indicated concentrations of Taxol for 18 h. *B*, A549 cells were exposed to 2 μM geldanamycin and to the indicated concentrations of Taxol for 18 h. Fifteen μg of total cell protein were separated by electrophoresis, transferred to nitrocellulose, and immunoblotted with either an anti-$p21^{WAF-1}$ polyclonal antibody or anti-p53 monoclonal antibody, as described in "Materials and Methods."

ever an accumulation of cells in G_2-M and a reduction of cells in G0/G1 cells was observed. There was no effect of geldanamycin on the G_2-M block induced by 12, 100, or 250 nM Taxol (data not shown).

Microtubule Organization. To determine the effects of low concentrations of Taxol on the subcellular organization of microtubules, the microtubule cytoskeleton was examined by immunofluorescence. Alterations in the normal microtubule cytoskeleton were observed even at concentrations of Taxol (1–9 nM) that were not sufficient to induce a G_2-M block (Fig. 5). A significant change in the microtubule network can be observed after incubation with low concentrations of Taxol (Fig. 5*B*). For example, treatment of A549 cells with 3 nM Taxol resulted in a partial parallel alignment of microtubules (Fig. 5*C*). At 5 nM Taxol, in addition to parallel alignment of microtubules in 30% of the cells, formation of bundles of microtubules was observed (Fig. 5*D*). At 12–250 nM Taxol, microtubule bundles were present at a highly significant level (Fig. 5*E*). Mitotic cells exposed to low Taxol concentrations (≤10 nM) developed multiple asters in a concentration-dependent manner. The latter may lead to asymmetrical cell division and be responsible for the formation of cells with an abnormal size and DNA content (Fig. 5*F*).

Subcellular Organization. At low Taxol concentrations in which cells are not blocked at G_2-M, they may undergo abnormal mitosis. To explore this idea, the morphology of the cells was examined after an 18-h exposure to Taxol. A549 cells revealed two aberrant cell types: multinucleated and apoptotic (Fig. 6). Untreated cells were generally uniform in size and had a single nucleus that was round in shape (Fig. 6*A*, *panel a*). After Taxol treatment, cells appeared multinucleated (Fig. 6*A*, *panel b*), and the percentage of such cells increased between 1–7 nM Taxol (Table 1). These multinucleated cells were distinguished from apoptotic cells (Fig. 6*A*, *panel c*) because they contained evenly stained nuclear fragments. At concentrations <9 nM, mitotic cells demonstrating abnormal DNA division were observed; Fig. 6*A*, *panel d* represents a cell during anaphase, in which one chromosome is not migrating with the rest of the other chromosomes (*arrow*). At 12 nM drug, 26% of the cells displayed the morphological characteristics of apoptosis: cell shrinkage, vacuolated cytoplasm, and regions of intense chromatin staining around the nuclear periphery (Fig. 6*A*, *panel c*; Table 1). At concentrations >12 nM, 40–50% of the cells were in mitosis (Table 1) and were blocked in metaphase.

Fig. 1 demonstrates the presence of hypodiploid cells after treatment with low Taxol concentrations (3–5 nM), whereas Table 1 demonstrates a low percentage of apoptotic cells and a significant induction of multinucleated cells (3–7 nM). Due to an apparent discrepancy between the results presented in Fig. 1 and Table 1, the hypodiploid cells observed by flow cytometry were isolated and analyzed by microscopy. The hypodiploid cells presented with two morphologies; multinucleated and apoptotic (Fig. 6*B*), the majority (>80%) being multinucleated. Thus, the multinucleated cells observed in Table 1 (3–5 nM) are actually hypodiploid cells. DNA ladders were not observed after the 18-h treatment with 5 nM Taxol, although they became visible after 24 h (data not shown). This suggested that cells containing an abnormal DNA content, in this case multinucleated cells, subsequently died by apoptosis.

Induction of Cell Death after Incubation with Low Concentrations of Taxol. The presence of hypodiploid cells observed in the cell cycle experiments done after drug treatment, prompted us to determine their cell viability. Cells were collected and stained with trypan blue to differentiate live cells from dead cells, as described in "Materials and Methods." Three types of cells were observed by microscopy: (*a*) trypan blue negative cells with normal morphology and size; (*b*) trypan blue negative cells with an approximate 50% reduction in size; and (*c*) trypan blue positive cells (Table 2). Low concentrations of Taxol (3–7 nM) did not induce a significant number of trypan blue positive cells after an 18-h treatment. However, 15% of the cells, after Taxol treatment (5–7 nM) for 18 h, showed a substantial (50%) reduction in size. At the same concentrations, 10% of the cells were multinucleated and enlarged with a diameter at least twice that of the control cells (data not shown). Because the small cells observed were trypan blue negative, we decided to prolong the period of incubation to see if these cells were predisposed to die.

Drug exposure (5–7 nM) for 24 h, resulted in a 15% cell death. However, small cells (trypan blue negative) were not observed at 24 h,

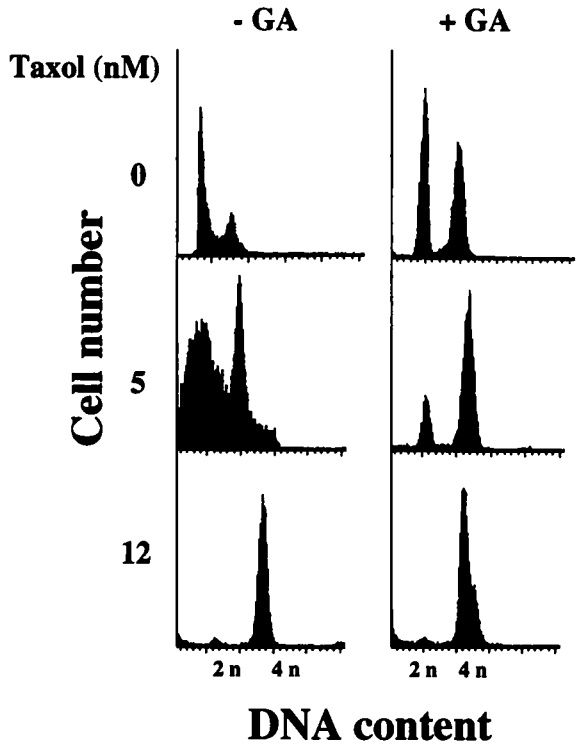

Fig. 4. Depletion of Raf-1 induces an accumulation of cells in G_2-M at low Taxol concentrations. A549 cells were incubated with either 5 or 12 nM Taxol in the presence or absence of geldanamycin (*GA*). Cells were collected after 24 h, fixed, stained with propidium iodide, and analyzed by flow cytometry, as described in "Materials and Methods."

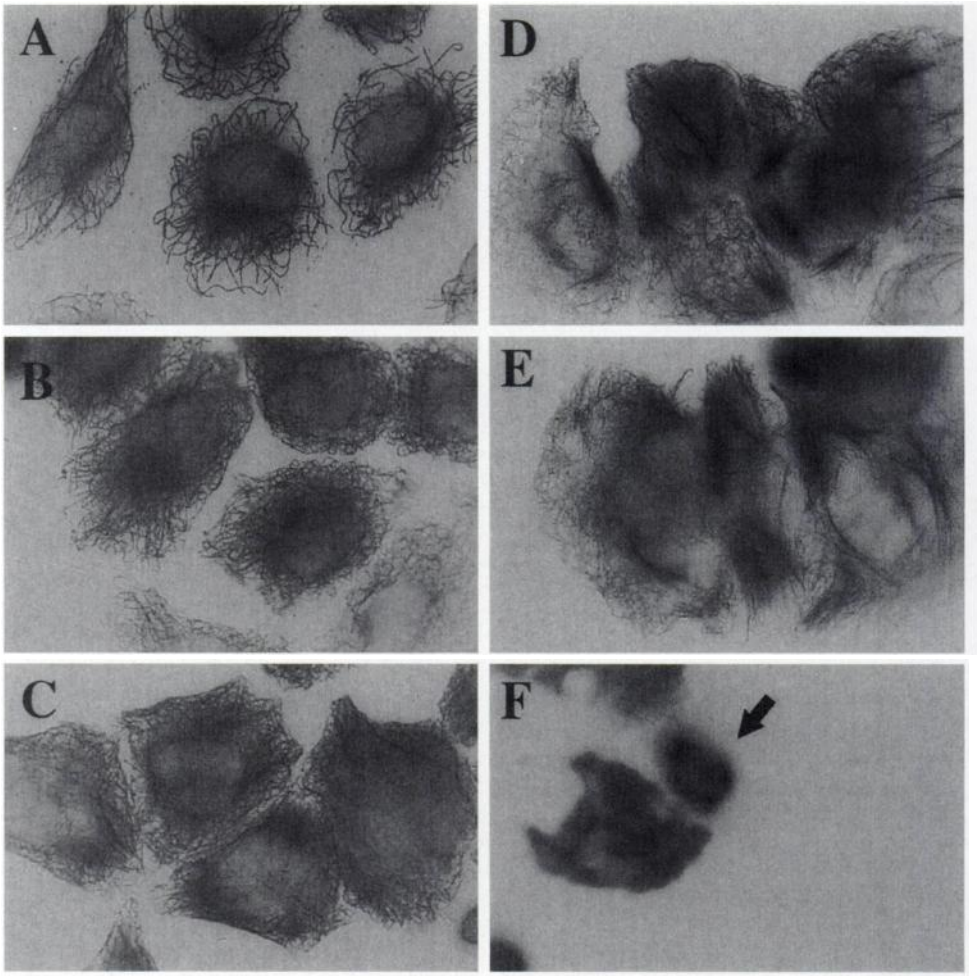

Fig. 5. Low concentrations of Taxol induce disruption of the normal microtubule cytoskeleton. A549 cells were exposed to varying concentrations of Taxol for 18 h. Cells were fixed and incubated with a β-tubulin antibody, as described in "Materials and Methods." *A*, untreated; *B*, 1 nM; *C*, 3 nM; *D*, 5 nM; *E*, 12 nM Taxol; *F*, a mitotic cell with multiple asters after treatment with 7 nM Taxol.

suggesting that the increase in cell death resulted from the death of those cells with an abnormally small size that were present after the 18-h drug treatment. The abnormalities observed in cell size and DNA division after Taxol treatment (5–7 nM), suggest that cells may not be blocked in G_2-M, but rather undergo an abnormal mitosis. At higher concentrations (>9 nM), cells did not display abnormalities in size, suggesting that cells undergo apoptosis directly after being blocked in G_2-M. Apoptosis induced by 5 and 12 nM Taxol after a 24-h incubation was confirmed by the presence of DNA ladders (data not shown).

DISCUSSION

This study has demonstrated that Raf-1 activation correlates with an accumulation of cells in the G_2-M phase of the cell cycle, indicating that Raf-1 may have a role in the passage through mitosis. In addition, it is clear that Taxol-mediated cell death may occur by different mechanisms; at low Taxol concentrations (<9 nM), cell death may result from an aberrant mitosis by a Raf-1-independent pathway, whereas, at higher Taxol concentrations, cell death may occur as a result of a terminal mitotic arrest, in a Raf-1-dependent manner.

Emphasis has been placed on the activation of Raf-1 kinase in the induction of apoptosis by Taxol, and it has been suggested that this activation is a consequence of the microtubule disruption induced by the drug (15, 16). Dead cells (15%) were observed in the absence of Raf-1 activation after a 24-h incubation with low concentrations of Taxol, indicating that Raf-1 activation is not a requirement for cell death. It has been shown that after higher doses of Taxol treatment in MCF7 cells, apoptosis is accompanied by Raf-1 activation (15). Taxol-induced cell death may result from the activation of different signal transduction pathways, depending on drug concentration.

Alterations in the microtubule network were observed even at concentrations of Taxol (<9 nM) that were not sufficient to induce a G_2-M block. These data indicate that the interaction of Taxol with microtubules is not sufficient to induce Raf-1 activation and that a critical level of microtubule disruption is required. A correlation between cell cycle disruption and Raf-1 activation was observed because the latter coincided with the accumulation of cells in G_2-M. The minimum Taxol concentration required for Raf-1 activation coincides with the minimum drug concentration needed to induce a G_2-M block.

The electrophoretic retardation of Raf-1 from mitotic cells indicates that Raf-1 modification occurs not only in response to Taxol treatment, but also during mitosis. Studies have shown that the morphology of cells is similar among those undergoing apoptosis, mitosis, and mitotic catastrophe, suggesting that the underlying biochemical changes during these processes may be related (24). Depletion of Raf-1 by geldanamycin in cells causes an accumulation of cells in the G_2-M phase, indicating that Raf-1 activation is important for the passage through mitosis. Previous studies have also presented evidence indicating a role for Raf-1 during mitosis (20, 21, 25). Using *Xenopus* oocytes, it was noted that Raf-1 kinase activity was increased 5–10-fold during metaphase (26). Our data confirm previous studies that show that Taxol-induced mitotic cells are blocked in the metaphase-anaphase boundary (8). The mitotic spindle checkpoint inhibits postmetaphase events in the absence of the proper alignment of

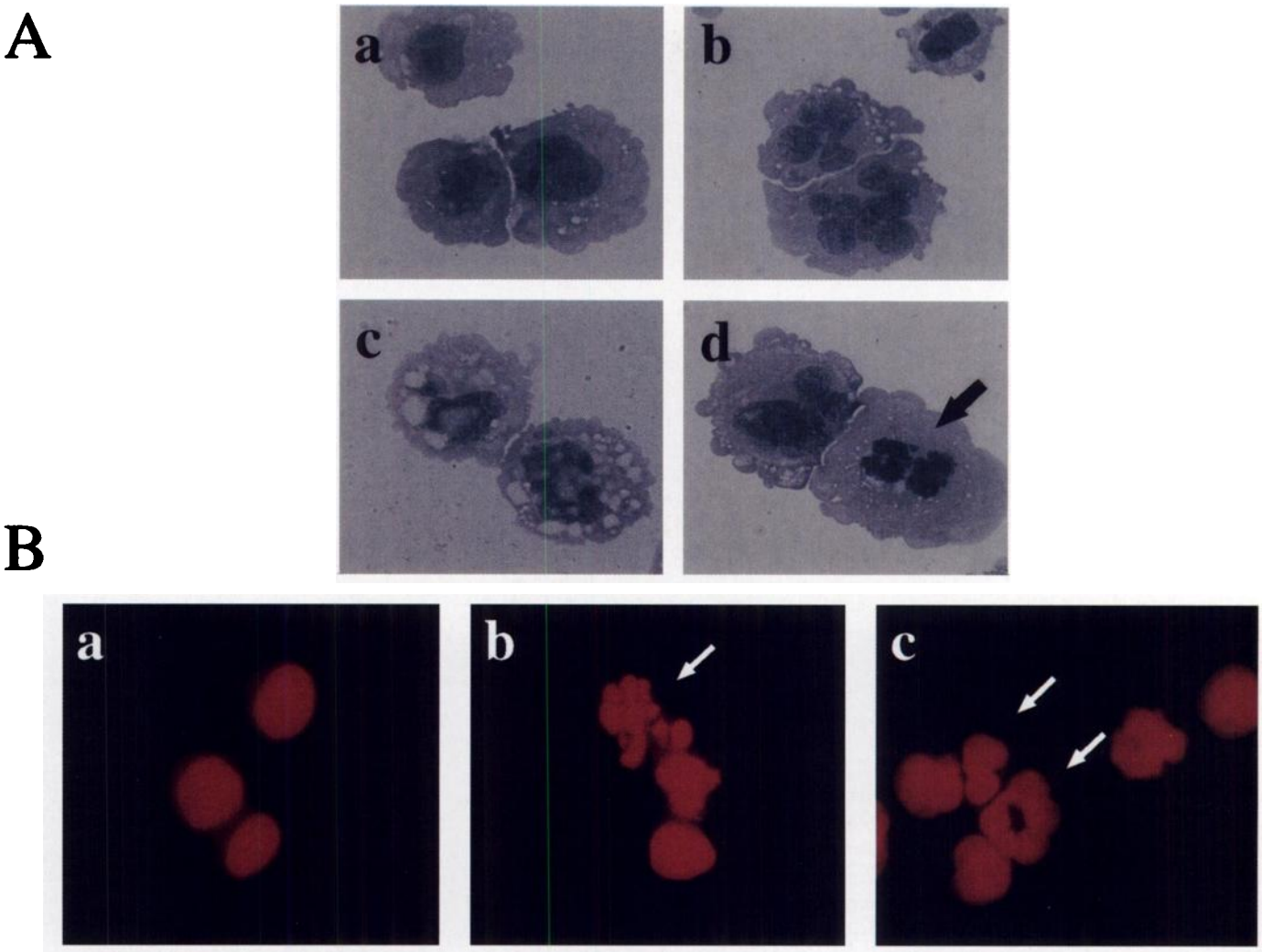

Fig. 6. *A*, morphological examination of A549 cells after an 18-h exposure to Taxol revealed two aberrant cell types: multinucleated and apoptotic cells. After drug treatment, all of the cells (adherent and nonadherent) were harvested. To determine the proportion of apoptotic, multinucleated and mitotic cells, 10,000 cells were spun onto a microscope slide and stained with Wright/Giemsa, as described in "Materials and Methods." *a*, control; *b*, multinucleated cells. Enlarged cells that contained multiple evenly stained nuclear fragments were considered to have undergone multinucleation; *c*, apoptotic cells. Cells that were shrunken and contained vacuolated cytoplasm and regions of intense chromatin staining were scored as apoptotic; *d*, anaphase cell. One chromosome is not migrating with the rest (*arrow*). *B*, the hypodiploid cells were isolated as described in "Materials and Methods." *a*, control; *b*, apoptotic cell (*arrow*); *c*, multinucleated cell (*arrow*).

Table 1 *Quantitation of mitotic, multinucleated, and apoptotic cells after Taxol treatment for 18 h*

The percentage of cells in each category was determined by morphologic analysis as described in "Materials and Methods." A minimum of 1000 cells/experiment were counted. Data presented are the means of two separate experiments, each one done in duplicate.

Taxol concentration (nM)	Mitotic cells (%)	Multinucleated cells (%)	Apoptotic cells (%)
0	1.3 ± 0.4	0.7 ± 0.2	0.0 ± 0.0
1	2.8 ± 0.2	9.5 ± 3.0	4.2 ± 1.7
3	1.5 ± 0.4	26.7 ± 8.0	3.5 ± 0.6
5	3.6 ± 0.2	42.0 ± 4.4	5.4 ± 2.0
7	7.1 ± 1.3	37.7 ± 5.5	15.7 ± 2.9
9	12.8 ± 3.2	34.3 ± 1.3	23.6 ± 4.5
12	21.6 ± 0.1	30.2 ± 4.4	25.9 ± 1.1
48	41.9 ± 3.8	10.1 ± 1.0	13.0 ± 0.1
100	42.1 ± 4.0	9.4 ± 0.7	16.5 ± 4.0
250	48.4 ± 1.4	6.7 ± 0.7	10.6 ± 1.5

chromosomes (27). The binding of Taxol to microtubules interrupts normal spindle formation, resulting in a block at the mitotic checkpoint. The mechanism by which the mitotic checkpoint inhibits progression through the cell cycle is not clear and Raf-1 activation may be a component of the signal cascade activated during the mitotic checkpoint.

It is known that Raf-1 interacts with important players in the mitotic checkpoint and with proteins involved in mitosis. For example, Raf-1 interacts with Cdc25A, which is involved in regulating the G_2-M transition (26). It has been shown also that Raf-1 activation is de-

Table 2 *Cytotoxicity of Taxol in A549 cells*

The percentage of cells in each category was determined by morphological analysis as described in "Materials and Methods." A minimum of 500 cells/experiment were counted. Data presented are the means of three separate experiments, each one done in duplicate.

Taxol (nM)	Time (h)	Trypan blue positive cells (%)	Trypan blue negative small cells (%)
0	18	4.8 ± 1.1	0.0 ± 0.0
3	18	2.0 ± 0.5	3.8 ± 1.0
5	18	3.8 ± 2.0	14.6 ± 0.3
7	18	3.7 ± 1.8	14.9 ± 0.2
12	18	2.7 ± 0.0	8.4 ± 0.0
100	18	5.8 ± 0.4	0.0 ± 0.0
250	18	6.3 ± 0.7	0.0 ± 0.0
0	24	7.4 ± 1.3	0.0 ± 0.0
3	24	3.6 ± 0.8	0.5 ± 0.2
5	24	14.9 ± 1.6	0.7 ± 0.3
7	24	14.7 ± 1.5	0.8 ± 0.5
12	24	23.6 ± 1.9	0.9 ± 0.1
100	24	22.9 ± 0.9	0.0 ± 0.0
250	24	21.0 ± 2.3	0.0 ± 0.0

pendent on the presence and selective association with a mitotic form of Lck in T cells (25). Raf-1 phosphorylates p53 *in vitro*, suggesting that p53, which has been implicated in a G_2-M checkpoint, may also be activated by Raf-1 *in vivo* (28, 29). A previous study (15) concluded that Raf-1 activation was not due to a G_2-M block because cells blocked in G2 after orthovanadate treatment, did not demonstrate Raf-1 activation. However, in human T cells, it has been demonstrated that Raf-1 is downstream of several signal transduction events, including the activation of a tyrosine phosphatase (30). Orthovanadate is a tyrosine phosphatase inhibitor, and it is not known if an upstream tyrosine phosphatase activity is required for activation of Raf-1.

A dose-dependent induction of p53 and $p21^{WAF-1}$ was observed in our studies. The increase in p53 and $p21^{WAF-1}$ correlated with the increase in hypodiploid cells observed by flow cytometry suggesting a role for $p21^{WAF-1}$ and p53 in mediating at least some of the cellular effects of low concentrations of Taxol. DNA damage results in induction of p53, followed by a G1 arrest that is believed to be mediated by $p21^{WAF-1}$ (31). The morphological studies showed that low concentrations of Taxol induced abnormal chromosome segregation. Induction of both proteins could be due to an unequal DNA segregation. The tumor suppressor p53 also has been identified to have a role during the mitotic checkpoint. Therefore, its induction could represent a response to abnormalities in the mitotic spindle. Previous studies have indicated that p53 and $p21^{WAF-1}$ induction by higher Taxol concentrations are Raf-1-dependent (22). We found that at low Taxol concentrations, p53 and $p21^{WAF-1}$ were induced independently of Raf-1, suggesting that a different pathway is activated at these low concentrations of Taxol.

Previous studies have suggested that low Taxol concentrations act by retarding or inhibiting progression through mitosis, thus altering microtubule dynamics rather than increasing the microtubule polymer mass (7, 8). Microtubule dynamics is an inherent part of the spindle formation and alignment of chromosomes. Taxol may cause dysfunctional spindles that cannot properly polymerize, therefore, affecting chromosome segregation. The interaction of Taxol with microtubules at low concentrations affects these important steps during mitosis, resulting in an abnormal segregation of chromosomes and an aberrant cytokinesis. The latter results in cells with abnormal size and DNA content, eventually causing cell death. The presence of multinucleated cells and cells with a substantial reduction in size, indicates that cells exit from mitosis abnormally. Exposure of cells to low Taxol concentrations may be sufficient to delay mitotic progression, but insufficient to induce a mitotic arrest. Our data confirm previous time-lapse studies that have indicated that cells exposed to Taxol attempt to complete mitosis; however, cytokinesis is inhibited and cells become multinucleated (32). At concentrations sufficient to block cells in the G_2-M phase, the interaction of Taxol with microtubules affects the cell cycle by completely blocking the progression of cells through mitosis, resulting in apoptosis. Both mechanisms of Taxol-mediated apoptosis require exit from mitosis.

In summary, Taxol induces different signal transduction pathways depending on the drug concentration. At high ($\geq$9 nM) Taxol concentrations, A549 cells are blocked in the G_2-M phase, resulting in cell death by a Raf-1-dependent pathway. At low (<9 nM) Taxol concentrations, A549 cells undergo an abnormal mitosis, resulting in the formation of multinucleated cells of which 15% subsequently die after 24 h by a Raf-1-independent mechanism.

ACKNOWLEDGMENTS

We thank David Gebhard for generous and expert assistance in flow cytometry and Dr. R. Britten for helpful discussions concerning the kinase assay.

REFERENCES

1. Rowinsky, E. K., and Donehower, R. C. Paclitaxel (Taxol). N. Engl. J. Med., *332:* 1004–1014, 1995.
2. Manfredi, J. J., Parness, J., and Horwitz, S. B. Taxol binds to cellular microtubules. J. Cell Biol., *94:* 688–696, 1982.
3. Schiff, P. B., Fant, J., and Horwitz, S. B. Promotion of microtubule assembly *in vitro* by Taxol. Nature (Lond.), *277:* 665–667, 1979.
4. Rao, S., Horwitz, S. B., and Ringel, I. Direct photoaffinity labeling of tubulin with Taxol. J. Natl. Cancer Inst., *84:* 785–788, 1992.
5. Rao, S., Krauss, N. E., Heerding, J. M., Swindell, C. S., Ringel, I., Orr, G. A., and Horwitz, S. B. 3′-(p-azidobenzamido)taxol photolabels the N-terminal 31 amino acids of β-tubulin. J. Biol. Chem., *269:* 3132–3134, 1994.
6. Schiff, P. B., and Horwitz, S. B. Taxol stabilizes microtubules in mouse fibroblast cells. Proc. Natl. Acad. Sci. USA, *77:* 1561–1565, 1980.
7. Jordan, M. A., Toso, R. J., Thrower, D., and Wilson, L. Mechanism of mitotic block and inhibition of cell proliferation by Taxol at low concentrations. Proc. Natl. Acad. Sci. USA, *90:* 9552–9556, 1993.
8. Jordan, M. A., Wendell, K., Gardiner, S., Derry, W. B., Copp, H., and Wilson, L. Mitotic block induced in HeLa cells by low concentrations of paclitaxel (Taxol) results in abnormal mitotic exit and apoptotic cell death. Cancer Res., *56:* 816–825, 1996.
9. Ding, A. H., Porteu, F., Sanchez, E., and Nathan, C. F. Shared actions of endotoxin and Taxol on TNF receptors and TNF release. Science (Washington DC), *248:* 370–372, 1990.
10. Bogdan, C., and Ding, A. Taxol, a microtubule-stabilizing antineoplastic agent, induces expression of tumor necrosis factor α and interleukin-1 in macrophages. J. Leukoc. Biol., *52:* 119–121, 1992.
11. Burkhart, C. A., Berman, J. W., Swindell, C. S., and Horwitz, S. B. Relationship between the structure of Taxol and other taxanes on induction of tumor necrosis factor-α gene expression and cytotoxicity. Cancer Res., *54:* 5779–5782, 1994.
12. Liu, Y., Bhalla, K., Hill, C., and Priest, D. G. Evidence for involvement of tyrosine phosphorylation in Taxol-induced apoptosis in a human ovarian tumor cell line. Biochem. Pharmacol., *48:* 1265–1272, 1994.
13. Wolfson, M., Yang, C. H., and Horwitz, S. B. Taxol induces tyrosine phosphorylation of shc and its association with grb2 in murine Raw 264.7 cells. Int. J. Cancer, *70:* 248–252, 1997.
14. Bhalla, K., Ibrado, A. M., Tourkina, E., Tang, C., Mahoney, M. E., and Huang, Y. Taxol induces internucleosomal DNA fragmentation associated with programmed cell death in human myeloid leukemia cells. Leukemia (Baltimore), *7:* 563–568, 1993.
15. Blagosklonny, M. V., Schulte, T., Nguyen, P., Trepel, J., and Neckers, L. M. Taxol-induced apoptosis and phosphorylation of Bcl-2 protein involves c-Raf-1 and represents a novel c-Raf-1 signal transduction pathway. Cancer Res., *56:* 1851–1854, 1996.
16. Blagosklonny, M. V., Giannakakou, P., el-Deiry, W. S., Kingston, D. G., Higgs, P. I., Neckers, L., and Fojo, T. Raf-1/bcl-2 phosphorylation: a step from microtubule damage to cell death. Cancer Res., *57:* 130–135, 1997.
17. Morrison, D. K., and Cutler, R. E. J. The complexity of Raf-1 regulation. Curr. Opin. Cell Biol., *9:* 174–179, 1997.
18. Lock, R. B., Galperina, O. V., Feldhoff, R. C., and Rhodes, L. J. Concentration-dependent differences in the mechanisms by which caffeine potentiates etoposide cytotoxicity in HeLa cells. Cancer Res., *54:* 4933–4939, 1994.
19. Wartmann, M., and Davis, R. J. The native structure of the activated Raf protein kinase is a membrane-bound multi-subunit complex. J. Biol. Chem., *269:* 6695–6701, 1994.
20. Laird, A. D., Taylor, S. J., Oberst, M., and Shalloway, D. Raf-1 is activated during mitosis. J. Biol. Chem., *270:* 26742–26745, 1995.
21. Lovri'c, J., and Moelling, K. Activation of Mil/Raf protein kinases in mitotic cells. Oncogene, *12:* 1109–1116, 1996.
22. Blagosklonny, M. V., Schulte, T. W., Nguyen, P., Mimnaugh, E. G., and Trepel, J. Taxol induction of $p21^{waf1}$ and p53 requires c-raf-1. Cancer Res., *55:* 4623–4626, 1995.
23. Schulte, W. T., Blagosklonny, M. V., Ingui, C., and Neckers, L. Disruption of the Raf-1-Hsp90 molecular complex results in destabilization of Raf-1 and loss of Raf-1-Ras association. J. Biol. Chem., *270:* 24585–24588, 1995.
24. King, K. L., and Cidlowski, J. A. Cell cycle and apoptosis: common pathways to life and death. J. Cell. Biochem., *58:* 175–180, 1995.
25. Pathan, N. I., Ashendel, C. L., Geahlen, R. L., and Harrison, M. L. Activation of T cell Raf-1 at mitosis requires the protein-tyrosine kinase Lck. J. Biol. Chem., *271:* 30315–30317, 1996.
26. Galaktionov, K., Jessus, C., and Beach, D. Raf1 interaction with Cdc25 phosphatase ties mitogenic signal transduction to cell cycle activation. Genes Dev., *9:* 1046–1058, 1995.
27. Glotzer, M. Mitosis: don't get mad, get even. Curr. Biol., *6:* 1592–1594, 1996.
28. Jamal, S., and Ziff, E. B. Raf phosphorylates p53 *in vitro* and potentiates p53-dependent transcriptional transactivation *in vivo*. Oncogene, *10:* 2095–2101, 1995.
29. Cross, S. M., Sanchez, C. A., Morgan, C. A., Schimke, M. K., Ramel, S., Idzerda, R. L., Raskind, W. H., and Reid, B. J. A p53-dependent mouse spindle checkpoint. Science (Washington DC), *267:* 1353–1356, 1995.
30. Siegel, J. N., June, C. H., Yamada, H., Rapp, U. R., and Samelson, L. E. Rapid activation of C-Raf-1 after stimulation of the T-cell receptor or the muscarinic receptor type 1 in resting T cells. J. Immunol., *151:* 4116–4127, 1993.
31. Ewen, M. E., and Miller, S. J. p53 and translational control. Biochim. Biophys. Acta, *1242:* 181–184, 1996.
32. Pulkkinen, J. O., Elomaa, L., Joensuu, H., Martikainen, P., Servomaa, K., and Grenman, R. Paclitaxel-induced apoptotic changes followed by time-lapse video microscopy in cell lines established from head and neck cancer. J. Cancer Res. Clin. Oncol., *122:* 214–218, 1996.